# Wireless-Powered Machine-to-Machine Multicasting in Cellular Networks

Abdullah M. Almasoud and Ahmed E. Kamal, Fellow, IEEE

Abstract—In future cellular networks, it is expected that data traffic will increase significantly due to deployments of large numbers of Internet of Things (IoT) objects. The IoT objects operate underlaying a cellular network, and they use Machine-to-Machine (M2M) communication to transmit multicst messages. We propose to use Radio Frequency (RF) Energy Transmitters (ET) to compensate the IoT objects with the energy consumed in forwarding multicast messages. Our goal is to support multicast service for IoT objects and transmit energy to them such that the total transferred energy by the ETs is minimized. We formulated the problem mathematically as a non-convex Mixed Integer Nonlinear Program (MINLP). Due to the difficulty of solving the problem optimally, we decompose the original problem into two sub-problems using Generalized Bender Decomposition with Successive Convex programming (GBD-SCP). Although this method facilitates finding a solution for the problem, the problem is still hard due to binary variables. Hence, we propose the Constraints Decomposition with SCP and Binary Variable Relaxation (CDR) algorithm to solve the problem more efficiently. Simulation results show that the proposed algorithm achieves a performance close to the GBD-SCP algorithm while the computation time is reduced significantly when the network size is larger.

*Index Terms*—Wireless-powered, energy harvesting, power transfer, multicast, M2M communication, routing, scheduling.

#### I. INTRODUCTION

ULTICASTING is an essential service for disseminating a message to a group of recipients. Instead of sending a message from a source to a group of destinations multiple times using unicast communications, multicast service allows addressing a message to a group of destinations simultaneously. Multicast service becomes more appealing in cellular networks due to a rapid growth in data traffic in the recent years [1]. Multicasting in current cellular

Manuscript received August 30, 2019; revised February 5, 2020; accepted March 30, 2020. Date of publication April 8, 2020; date of current version May 19, 2020. This work was supported in part by the National Science Foundation, USA, under Grant 1827211; and in part by the Deanship of Scientific Research at Prince Sattam bin Abdulaziz University, Alkharj, Saudi Arabia. The associate editor coordinating the review of this article and approving it for publication was E. Ayanoglu. This article was presented in part at the 2018 IEEE Global Communications Conference. (Corresponding author: Abdullah M. Almasoud.)

Abdullah M. Almasoud was with the Department of Electrical and Computer Engineering, Iowa State University, Ames, IA 50011 USA. He is now with the Department of Electrical Engineering, College of Engineering, Prince Sattam bin Abdulaziz University, Al-Kharj 11942, Saudi Arabia (e-mail: am.almasoud@psau.edu.sa).

Ahmed E. Kamal is with the Department of Electrical and Computer Engineering, Iowa State University, Ames, IA 50011 USA (e-mail: kamal@iastate.edu).

Digital Object Identifier 10.1109/TGCN.2020.2986216

networks is used for content delivery for typical cellular phones. However, with the revolution of the Internet of Things (IoT), Machine-to-Machine (M2M) multicast service for large numbers of low-power IoT devices in cellular networks is required. Therefore, we need to consider several challenges while supporting this emerging type of multicast service.

IoT is a technology that enables physical objects to observe and monitor activities and phenomena, processes the collected data and communicate with other physical objects in order to make a decision or accomplish a certain task [2]. It is expected that the number of IoT objects that will be deployed in the world will reach 50 billions by 2020 [3]. M2M communication, which is also called machine-type-communication (MTC), is considered as an important enabling technology for IoT, where it allows direct communication between neighboring IoT objects.

Multicasting over cellular networks can be classified based on its applications into human oriented and machine oriented [4]. Multicast service in cellular networks is developed typically for human-based applications like video content delivery. On the other hand, machine oriented multicast is designed to support multicast service for machine-based applications, which includes: 1) An IoT object sends software updates to a group of IoT objects; 2) an IoT object sends a multicast messages to a group of IoT actuators to perform controlling actions in a factory; and 3) an IoT sensing object that detects hazardous events on the road and multicast warning messages to a groups of IoT objects embedded in Vehicular Ad Hoc Networks (VANET). Therefore, machine oriented multicasting should address the challenges associated with IoT to enable its applications in the next generation of the cellular networks.

IoT devices are typically designed to use small size batteries to satisfy their energy demands. On the other hand, devices in wireless-powered networks harvest RF (Radio Frequency) energy from dedicated energy transmitters or from ambient RF radiation. RF energy harvesting is a technology that enables converting a received RF signal to energy [5]. Hence, wireless-powered network has emerged as a candidate solution for some applications in future networks [6]. Although wireless energy transfer gives the IoT devices an efficient way to satisfy their energy demands without the need for battery replacement, a significant portion of the transmitted signal for charging is wasted because of signal attenuation and non-optimality of the energy harvesters.

There is a trade-off between satisfying the energy demands of the IoT devices using only wireless energy transfer or

2473-2400 © 2020 IEEE. Personal use is permitted, but republication/redistribution requires IEEE permission. See https://www.ieee.org/publications/rights/index.html for more information.

batteries. The former approach helps the IoT to satisfy their energy demands without the need for battery replacement or suffering from energy outage. However, part of the transmitted energy can be lost due to the warless medium and imperfect energy harvesters. Therefore, using only conventional batteries to power IoT devices eliminates wasting energy that happens during wireless energy transfer. Accordingly, it may not be feasible to power the whole M2M devices (IoT objects) in the network using only RF energy harvesting technology. However, wireless energy transfer can power the M2M devices partially by supporting the M2M devices with the required energy to transmit the multicast messages.

In this paper, we consider wirelessly powered M2M multicasting underlaying cellular networks. Due to the high cost of powering the multicast communication using wireless energy transfer, the goal is that we minimize the total required energy to be transferred from the Energy Transmitters (ET) to the M2M devices. Since M2M devices are compensated for the energy consumed in sending multicast messages, they should minimize their total consumed energy for transmission to reduce the total transmitted energy from the ETs. As the M2M devices operate underlaying a cellular network, they must keep their interference under certain thresholds to protect the regular cellular users and the other M2M devices. Within any time slot, the M2M devices can either: 1) transmit data; 2) receive data; 3) harvest energy; or 4) stay idle. Hence, we show how to schedule multicast message transmission and reception and RF energy harvesting for the M2M devices. The scheduling process aims in supporting the multicast services while minimizing the required transmitted energy by the ETs.

#### A. Related Works

1) Wireless-Powered Networks: In [7], the authors studied the beamforming in multicast wirelessly powered networks. They formulated the problem mathematically and proposed a fast parallel iterative algorithm that converges to a KKT point. The paper in [8] considered energy efficiency optimization for machined-to-machined communication. The proposed work considered a joint optimization for channel selection, power control and time allocation. Moreover, the authors in [11] investigated maximum energy efficiency in wireless powered networks using dedicated power transmitters. They considered time allocation and power control jointly to maximize energy efficiency.

In [13], a framework for peer-harvesting in wireless-powered networks is introduced. A hybrid base station sends data and energy to a set of wireless nodes that can harvest energy from the hybrid base station and from each other. The proposed scheme specifies how the wireless-powered network allows a wireless node to harvest energy from its peers in addition to the hybrid base station.

2) Cellular Networks: Since energy harvesting from ambient energy sources may not always be feasible, the authors in [12] proposed to use dedicated power beacons to charge devices in wireless-powered cellular networks. A hybrid base station that sends data can also charge the devices in the cellular network in addition to the dedicated power beacons. They

demonstrated a significant improvement on the outage probability for the users when they are charged using dedicated power beacons rather than using ambient energy resources or a hybrid base station. In [10], the authors proposed an architecture and a model to transfer power wirelessly in cellular networks. They introduced what is called power beacons, which charge mobile devices using microwave radiation. They also investigated the deployment of the cellular network under an outage constraint on the data transmission link. In [14], the authors proposed a cellular IoT network that transfers energy to IoT devices and shares the spectrum of the cellular network opportunistically. The proposed work aimed at enhancing spectrum and energy efficiencies.

3) Internet of Things: In [16], we proposed a cognitive mobile base station that transmits data and energy to IoT devices. To transfer energy to the IoT devices within a certain tolerable time, the mobile base station adjusts its location and transmission power such that the IoT devices are charged without delay. To optimize the operation of the mobile base station, we showed how to minimize the total energy consumed in energy transfer and the mobility of the base station. The paper in [15] studied an energy efficient resource allocation for M2M communication and energy harvesting for IoT. Joint power allocation and time allocation are considered in order to minimize total energy consumption. The authors in [17] studied full-duplex M2M communication for wireless-powered IoT. The idea of the paper is to utilize the extra energy not used by receivers, and hence, receiving IoT devices transfer energy to the transmitting IoT device.

4) Multicasting: An M2M multicast service for transferring data and energy to a large number of users is proposed in [18]. It is shown that the proposed scheme reduces energy consumption and delay while reducing the control overhead. In [19], the authors introduced a reliable multicast and broadcast method for energy harvesting network. The proposed method guarantees reliable multicast service for the energy harvesting nodes which suffers from energy deficiency. In [20], algorithms for routing multimedia multicast in IoT is studied. It is shown that the speed and the accuracy of the proposed algorithm outperforms a representative multicast routing algorithm. Wireless-powered multicast and unicast services with full duplex self-energy recycling is investigated in [9]. The goal is to maximize the secrecy-multicast rate region subject to transmit power constraints.

#### B. Motivations and Contributions

When the M2M devices are small and battery powered, they tend to optimize their operations to prolong their batteries lifetimes. One important application of M2M communication is the multicast service, where a sender sends a message to a group of destinations. The multicast tree may include a multihop communication between the M2M devices, where M2M devices should be encouraged to participate in forwarding the multicast message. However, the M2M devices can operate in a greedy way and avoid collaborating in forwarding the multicast message. Therefore, we propose in this work to incentivize the M2M devices to collaborate in forwarding the multicast tree by charging them wirelessly using distributed

energy transmitters. To best of our knowledge, no paper in the literature discuss incentivizing the M2M devices to participate in multicast tree forwarding by charging them wirelessly.

The contributions of our paper can be summarized as follows:

- We formulate the problem of wireless-powered M2M multicasting in cellular network such that the total transmitted energy by ETs is minimized. We consider the routing and the scheduling of multicast messages and the scheduling of energy harvesting. The Base Station (BS) can contribute to forwarding the multicast messages to the destinations if that helps in minimizing the total transmitted energy.
- The formulated problem for finding the optimal solution is a non-convex Mixed Integer Nonlinear Program (MINLP). Therefore, it is difficult to obtain a solution efficiently. We use Generalized Bender Decomposition with Successive Convex Programming (GBDC-SCP) to find a solution for our problem. To facilitate the solution, we approximate the non-convex data rate function by a concave lower bound function. Then, we decompose the original problem into a convex Nonlinear Program (NLP) and Mixed Integer Linear Program (MILP) using Generalized Bender Decomposition (GBD) [21]. Moreover, we solve the NLP problem successively using Successive Convex Programming (SCP) within GBD.
- Although the GBD-SCP algorithm can find a solution for our problem after decomposing the problem into convex NLP and MILP subproblems, the problem is still hard to solve due to the binary variables in the MILP problem. Hence, we propose Constraints Decomposition with SCP and Binary Variable Relaxation (CDR) algorithm to solve the optimization problem. We show in this paper that each group of variables may depend on the solution of another group of variables. Hence, CDR algorithm decomposes the optimization problem into an LP and two NLP subproblems based on the dependence of the variables on each other. Moreover, all binary variable are relaxed to find a solution for the problem in a more efficient way. We show that the proposed algorithm converges to a solution within a finite number of iterations, and it reduces the computation time significantly when the network size is large.
- We study in the simulation section the performance of GBD-SCP and CDR algorithms and compare their computation times. We show that GBD-SCP slightly outperforms CDR algorithm, but CDR achieves a better performance in terms of computation time. Moreover, we compare the total energy consumption when ad hoc and hybrid network architectures are used. We show that the hybrid architectures can reduce the total needed wireless energy transfer compared with the ad hoc architectures.

#### C. Paper Organization

This paper is organized as follows. In Section II, we describe the system model, then we formulate the problem in Section III. We discuss how to solve the formulated problem

## TABLE I

Crimbal	Description		
Symbol	Description		
$\frac{C}{\overline{C}}$	The set of channels used by cellular and M2M devices.		
$\frac{c}{Z}$	The set of channels used for power transfer.  The set of time slots.		
S	The set of M2M users.		
BS	Base station.		
$\overline{S}$	$S \cup BS$ .		
P	The set of regular cellular network users.		
ET	Energy transmitter.		
$ET_i$	i <sup>th</sup> energy transmitter.		
ETS	Energy transmitters set.  The gain of channel c between node <i>i</i> and node <i>j</i> .		
$G_{ij}^c$ $PL_c$	Path loss constant for channel c.		
$PL_e$	Path loss exponent.		
$\alpha_c, \beta_c$	Fast and slow fading gains for channel c, respectively.		
$A_t, A_r$	Transmitting and receiving antenna gains, respectively.		
$d_{ij}$	Distance between node $i$ and node $j$ .		
$\phi, \phi$	$ET_i$ 's antenna azimuth and elevation angles in degree.		
$W, N_0$	Channel bandwidth and the noise spectral density.		
$P_i^{tx}(c,z)$	Transmission power of M2M device $i$ over channel $c$ and during slot $z$ .		
n ( = )	The point where $R_{ij}(c,z)$ function is approximated		
$P_i(c,z)$	around it using the first-order Taylor approximation.		
$P_{max}^{tx}$	Maximum transmission power of M2M devices.		
$P_i^{cell}(c,z)$	A parameter for the transmission power of the <i>i</i> <sup>th</sup> regular		
	cellular users to the BS over channel $c$ and during slot $z$ . Transmission power of $ET_e$ to M2M device $i$ over channel		
$P_{ei}^{ET}(c,z)$	c and during slot $z$ .		
$\frac{P_{max}^{ET}}{P^{BS}}$	Maximum transmission power for ETs.		
$P^{BS}$	Transmission power of the BS.		
W	Channel bandwidth.		
$\gamma_{ij}(c,z)$	The signal received by M2M $j$ from M2M $i$ , over channel		
	c and during slot z.  Data rate of the link between a transmitting M2M i to		
$R_{ij}(c,z)$	a receiver $j$ over channel $c$ and during slot $z$ .		
$\overline{R}_{ij}(c,z)$	Approximate data rate of the link between a transmitting		
Rij (c, z)	M2M $i$ to a receiver $j$ over channel $c$ and during slot $z$ .		
$P_{max}^h$	Maximum energy that the energy harvesting circuit can harvest.		
	Parameters used to model the nonlinearity of the energy		
ν, τ	harvesting circuit.		
$\Gamma^{EH}$	Sensitivity of the energy harvester.		
$\Gamma^{M2M}$	A threshold used to control SINR of M2M devices.		
$\Gamma^{cell}$	A threshold used to control interference to cellular devices.		
$X_i(c,z)$	A binary variable equals 1 only if M2M <i>i</i> transmits over channel <i>c</i> during slot <i>z</i> .		
	A binary variable equals 1 only if M2M <i>i</i> transmits to a		
$X_{ij}(c,z)$	receiver $j$ over channel $c$ during slot $z$ .		
$X_i^{cell}(c,z)$	A parameter equals 1 only if cellular user i transmits over		
i (c, z)	channel c during slot z.		
$H_i(c,z)$	A binary variable equals 1 only if M2M $i$ harvests energy over channel $c$ during slot $z$ .		
	A binary variable equals 1 only if M2M <i>i</i> harvests energy		
$H_{ei}(c,z)$	from $ET_e$ over channel $c$ during slot $z$ .		
990	An indicator equals 1 only if M2M $i$ is located within the		
$\mathbb{H}_{ei}^c$	energy harvesting zone of $ET_e$ that transmits power over channel $c$ .		
	A variable represents the data flow, in bits, of the link		
CY()	between a transmitting M2M i and a receiver j used to		
$\int_{ij}^{y}(c,z)$	route the multicast traffic, over channel $c$ and during slot		
	z, to destination y.		
$\frac{s}{d}$	The source of the multicast session.  The set of destinations for the multicast session.		
$\frac{a}{q}$	Required data demand by the multicast session in bits.		
T	slot duration.		
$E_i^{tx}(z)$	Energy consumed by M2M $i$ for transmission during slot $z$ .		
$E_i^H(z)$	Energy harvested by M2M i during slot z.		
$BL_i(z)$	Battery level of M2M i during slot z.		
BL <sup>min</sup>	Minimum battery level.		
$\frac{BL_i^{init}}{BL_i^{max}}$	Initial battery level of M2M <i>i</i> .  Maximum battery level of M2M <i>i</i> .		
	ivianimum dattery level of $vi \angle lvi$ $l$ .		

using GBD-SCP and CDR algorithms in Sections IV and V, respectively. We show and discuss the simulation results in Section VI. Finally, we conclude our paper in Section VII.

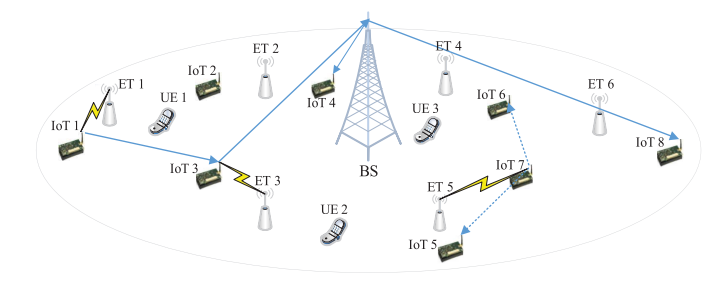


Fig. 1. M2M multicasting with energy harvesting in cellular networks.

#### II. SYSTEM MODEL

In this paper, we consider a set of M2M devices, S, operating underlaying the uplink bands of a cellular network. The M2M device can transmit over a set of channels, C, and it keeps its interference to the other M2M devices and to the set of regular cellular users, P, below certain thresholds  $\Gamma^{M2M}$  and  $\Gamma^{cell}$ , respectively. The Base Station (BS) can receive the multicast message from an M2M device and forward it to all destination M2M devices. A set of energy transmitters, ETS, transmit power wirelessly, over a set of channels  $\overline{C}$ , to all M2M devices engaged in multicast message transmission.

Multicast message transmission and energy harvesting for M2M devices are scheduled over a set of time slots, *Z*, where the duration of each time slot is *T*. M2M devices are equipped with batteries to perform their designated functions. However, energy consumed for multicast message transmission is compensated by transferring power wirlessly from ETs. M2M devices operate under harvest-use-store mode [22]. Therefore, each M2M device harvests energy, uses it in multicast messages transmission and stores in its battery only the unused harvested energy. ET with best channel condition to the M2M is used to transfer the power to minimize total transferred energy.

Fig. 1 shows a scenario for multicasting in IoT using M2M communication underlying a cellular network. IoT 1 transmits a multicast message to IoT 4 and IoT 8, whereas IoT 7 transmits a multicast message to IoT 5 and IoT 6. It is required to minimize total energy consumed for multicast message transmission in order to minimize total energy transmitted by ETs. Therefor, IoT 1 forwards its message to IoT 3 using M2M link to avoid transmitting with high power to the BS to deliver the message to the destinations. Then, IoT 3 forwards the multicast message to the BS, and the BS forwards the multicast message to IoT 4 and IoT 8. On the other hand, IoT 7 is located in close proximity to IoT 5 and IoT 6, and it consumes less energy when it multicasts directly to these destinations using M2M communication rather than reaching them through the BS. Hence, it multicasts the message directly to the destinations using M2M communication.

The gain of channel c between node i and node j,  $G_{ij}^c$ , is given by

$$G_{ij}^c = PL_c \ \alpha_c \ \beta_c \ A_t \ A_r \ d_{ij}^{-PL_e} \tag{1}$$

where  $PL_c$  is the path loss constant for channel c,  $PL_e$  is the path loss exponent,  $\alpha_c$  and  $\beta_c$  are fast and slow fading gains for channel c, respectively,  $A_t$  and  $A_r$  are transmitting and

receiving antenna gains, respectively, and  $d_{ij}$  is the distance between node i and node j. We assume that  $A_t = A_T = 1$  for M2M devices, whereas ETs use directional antennas for power transfer, and it is approximated by [23]

$$A_t \approx \frac{30,000}{\phi \,\overline{\phi}} \tag{2}$$

where  $\phi$  and  $\overline{\phi}$  are the antenna azimuth and elevation angles, respectively, in degree.

Let  $\mathbb{H}_{ei}^c$  be an indicator function equals 1 only if M2M device i is located within the energy harvesting zone of  $ET_e$  which transmits power over channel c. Hence,  $\mathbb{H}_{ei}^c$  function is given by

$$\mathbb{H}_{ei}^{c} = \begin{cases} 1, & d_{ei} \leq \left(\frac{P_{max}^{ET} P L_{c} \alpha_{c} \beta_{c} A_{t} A_{r}}{\Gamma^{EH}}\right)^{\frac{1}{PL_{e}}} \\ 0, & \text{otherwise} \end{cases}$$
(3)

where  $P_{max}^{ET}$  is maximum transmission power for each  $ET_i \in ETS$  and  $\Gamma^{EH}$  is minimum input power to the energy harvester to harvest energy.

M2M devices operate underlying a cellular network, and hence, regular cellular users cause interference to M2M devices' transmission. Let  $P_i^{tx}(c,z)$  be the transmission power of M2M device i over channel c and during slot z. The signal to noise plus interference ratio for the transmission of an M2M device to a receiver j is calculated as follows:

$$\gamma_{ij}(c,z) = \frac{P_i^{tx}(c,z) \ G_{ij}^c}{\sum_{q \in S \setminus i} P_q^{tx}(c,z) \ G_{qj}^c + N_j} \tag{4}$$

where  $N_j = \sum_{r \in P} P_r^{cell}(c,z)$   $G_{rj}^c + N_0 W$ ,  $P_r^{cell}(c,z)$  is transmission power of the  $r^{th}$  regular cellular users to the BS over channel c and during slot z,  $N_0$  is the noise spectral density and W is the channel bandwidth.

From equation (4), the data rate of a transmitting M2M device i to a receiving node j over channel c and during slot z is given by

$$R_{ij}(c,z) = W \log_2(1 + \gamma_{ij}(c,z))$$
(5)

The total harvested energy that M2M i can harvest from  $ET_k$  over channel c and during slot z,  $\eta_{ki}(c,z)$ , is given by [24], [25]

$$\eta_{ki}(c,z) = \left[ \frac{P_{max}^h}{e^{-\tau \Gamma^{EH} + v}} \left( \frac{1 + e^{-\tau \Gamma^{EH} + v}}{1 + e^{[-\tau P_{ki}^{ET}(c,z)G_{ki}^c + v]}} - 1 \right) \right]^+$$
(6)

where  $P_{ki}^{ET}(c,z)$  is the transmission power of  $ET_k$  to M2M device i over channel c and during slot z,  $P_{max}^h$  is the maximum harvested energy that the energy harvesting circuit can harvest,  $\Gamma^{EH}$  is the sensitivity of the energy harvester, v and  $\tau$  are parameters used to model the nonlinearity of the energy harvesting circuits and  $[x]^+ = \max(0, x)$ . Hence, the total energy consumed and harvested by user i during slot z are given, respectively, as follows:

$$E_i^{tx}(z) = \sum_{c \in C} P_i^{tx}(c, z) T \tag{7}$$

and

$$E_i^H(z) = \sum_{c \in \overline{C}} \sum_{k \in ETS} T \eta_{ki}(c, z). \tag{8}$$

#### III. PROBLEM FORMULATION

We assume that the M2M device is equipped with a single radio. Hence, the M2M device can either transmit, receive or harvest energy during each time slot, i.e.,

$$\sum_{c \in C} \left[ X_i(c, z) + \sum_{\forall k \in \overline{S}} X_{ki}(c, z) \right] + \sum_{c \in \overline{C}} H_i(c, z) \le 1,$$

$$\forall i \in S, z \in Z.$$
(9)

The binary variable  $X_{ij}(c,z)$  is set to 1 if there is a flow from M2M device i to a receiver j over channel c and during slot z, i.e., when  $0 < f^y_{ij}(c,z)$ , and it is set to 0 otherwise. Therefore, we have the following two constraints:

$$X_{ij}(c,z) \le \sum_{y=1}^{|d|} f_{ij}^y(c,z), \ \forall i \in S, j \in \overline{S}, \forall c \in C, z \in Z.$$

$$\tag{10}$$

$$\frac{f_{ij}^{y}(c,z)}{v} \le X_{ij}(c,z),$$

$$\forall i \in S, \quad j \in \overline{S}, c \in C, \quad y \in d, z \in Z.$$
(11)

The following two constraints set  $X_i(c, z)$  to 1 if  $\exists X_{ij}(c, z) = 1$  and set  $X_i(c, z)$  to 0 otherwise.

$$X_i(c,z) \le \sum_{j \in \overline{S}} X_{ij}(c,z), \ \forall i \in S, c \in C, z \in Z.$$
 (12)

$$\frac{\sum_{j\in\overline{S}}X_{ij}(c,z)}{|\overline{S}|} \le X_i(c,z), \forall i \in S, c \in C, z \in Z. \quad (13)$$

Similarly for  $H_i(c, z)$ , we have

$$H_i(c,z) \le \sum_{e \in ETS} H_{ei}(c,z), \ \forall i \in S, c \in \overline{C}, z \in Z.$$
 (14)

$$\frac{\sum_{e \in ETS} H_{ei}(c, z)}{|ETS|} \le H_i(c, z), i \in S, c \in \overline{C}, z \in Z.$$
 (15)

A receiver j can receive a message from an M2M device i over channel c and during slot z if  $\gamma_{ij}(c,z)$  is greater than a certain threshold  $\Gamma^{M2M}$ , i.e.,

$$\Gamma^{M2M} X_{ij}(c, z) \le \gamma_{ij}(c, z)$$

$$\forall i \in S, j \in \overline{S}, c \in C, z \in Z.$$
(16)

Let  $f_{ij}^y(c,z)$  be a variable representing data flow, in bits, of the link between a transmitting M2M i and a receiver j used to route the multicast traffic, over channel c and during slot z, to destination y. Since the flow over a certain link cannot exceed its capacity, we have

$$f_{ij}^{y}(c,z) \le R_{ij}(c,z)T,$$

$$\forall i \in S, \quad j \in \overline{S}, y \in d, c \in C, z \in Z.$$
(17)

Transmission power of the M2M device over a certain channel and during a time slot is zero when it is not scheduled for transmission over that channel and during that time slot. Therefore, it is upper bounded by the maximum transmission power,  $P_{max}^{tx}$ , as follows:

$$\chi P_i^{tx}(c,z) \le P_{max}^{tx} X_i(c,z), \quad \forall i \in S, c \in C, z \in Z.$$
 (18)

To satisfy a data flow demand, q, form the source of the multicast, s, to a set of destinations, d, the flow conservation constraints are given by

$$\sum_{z=1}^{|Z|} \sum_{c \in C} \sum_{i \in \overline{S} \setminus s} f_{is}^{y}(c, z) = 0, \quad \forall y \in d.$$
 (19)

$$\sum_{z=1}^{|Z|} \sum_{c \in C} \sum_{j \in \overline{S} \setminus y} f_{yj}^{y}(c, z) = 0, \quad \forall y \in d.$$
 (20)

$$\sum_{z=1}^{|Z|} \sum_{c \in C} \sum_{j \in \overline{S} \setminus s} f_{sj}^{y}(c, z) = q, \quad \forall y \in d.$$
 (21)

$$\sum_{z=1}^{|Z|} \sum_{c \in C} \sum_{i \in \overline{S} \setminus y} f_{iy}^{y}(c, z) = q, \quad \forall y \in d$$
 (22)

and

$$\sum_{z=1}^{|Z|} \sum_{c \in C} \sum_{n \in \overline{S} \setminus y} f_{ni}^{y}(c, z) = \sum_{z=1}^{|Z|} \sum_{c \in C} \sum_{j \in \overline{S} \setminus s} f_{ij}^{y}(c, z),$$

$$\forall i \in \overline{S} \setminus (s \cup y), \forall y \in d$$
(23)

where flow bifurcation is possible.

M2M devices can share channels with regular cellular users as long as they do not cause harmful interference to the signal transmitted by the regular cellular users. Therefore,

$$\Gamma^{cell} X_k^{cell}(c, z) \leq \frac{P_k^{cell}(c, z) G_{kb}^c}{\sum_{i \in S} P_i^{tx}(c, z) G_{ib}^c + N_0 W}$$

$$\forall k \in P, c \in C, z \in Z$$
(24)

where  $\Gamma^{cell}$  is a threshold used to control interference to cellular devices and  $X_k^{cell}(c,z)$  is a parameter equals 1 if cellular user i transmits over channel c during slot z and zero otherwise.

 $ET_e$  transmits power over channel c and during slot z to M2M device i only if that device is scheduled for receiving energy from  $ET_e$  over channel c and during slot z, i.e.,

$$P_{ei}^{ET}(c,z) \le P_{max}^{ET} H_{ei}(c,z),$$

$$\forall e \in ETS, \ \forall i \in S, \ \forall c \in C, z \in Z.$$
 (25)

To ensure that the M2M device participating in forwarding the multicast message is compensated for the energy consumed in transmission, we have

$$\sum_{z=1}^{|I|} E_i^{tx}(z) \le \sum_{z=1}^{|I|} E_i^H(z), \quad \forall i \in S.$$
 (26)

Based on the RF energy harvester implementation, the M2M device can harvest energy from a received signal if the input power is greater than a certain threshold,  $\Gamma^{EH}$ , i.e.,

$$\Gamma^{EH} H_{ei}(c,z) \leq P_{ei}^{ET}(c,z) G_{ei}^c$$

$$\forall e \in ETS, \forall i \in S, \forall c \in \overline{C}, z \in Z.$$
 (27)

Moreover, M2M device i needs to be located within the energy harvesting zone of an  $ET_e$  to be able to harvest energy from that ET, i.e.,

$$H_{ei}(c,z) \le \mathbb{H}_{ei}^c, \forall e \in ETS, i \in S, \forall c \in \overline{C}, z \in Z.$$
 (28)

Let the battery level of M2M device i during slot z be  $BL_i(z)$ , which is defined as follows:

$$BL_i(1) = BL_i^{init}, \quad \forall i \in S.$$
 (29)

$$BL_{i}(z) = BL_{i}(z-1) - E_{i}^{tx}(z) + E_{i}^{H}(z)$$
  
$$\forall i \in S, z \in Z \setminus 1$$
 (30)

where  $BL_{i}^{init}$  is initial battery level of M2M i.

The battery level does not exceed its maximum capacity, and cannot be negative. Therefore,

$$0 \le BL_i(z) \le BL_i^{max} \quad \forall i \in S, z \in Z \setminus 1.$$
 (31)

M2M device i cannot transmit if the battery energy level is below a threshold  $BL^{min}$ . Hence,

$$X_i(c,z) \le \frac{BL_i(z)}{BL^{min}}, \quad \forall i \in S, c \in C, z \in Z.$$
 (32)

The problem of minimizing the total transmitted energy from all ETs to M2M devices to support multicast communication is formulated as follows:

P1: Minimize: 
$$\sum_{e \in ETS} \sum_{i \in S} \sum_{c \in \overline{C}} \sum_{z=1}^{|I|} P_{ei}^{ET}(c, z) T \quad (33)$$

#### Subject to:

Constraints (9-24), (25-32).

$$X_{i}(c,z), X_{i,j}(c,z), H_{i}(\overline{c},z), H_{ei}(\overline{c},z) \in \{0,1\},$$

$$\forall i \in S, j \in \overline{S}, e \in ETS, c \in C, \overline{c} \in \overline{C}, z \in Z. \quad (34)$$

$$0 \leq f_{ij}^{y}(c,z) \leq v$$

$$\forall i, j \in \overline{S}, y \in d, c \in C, z \in Z. \tag{35}$$

$$0 \le P_i^{tx}(c, z) \le P_{max}^{tx}, \quad \forall i \in S, c \in C, z \in Z.$$
 (36)

$$0 \le P_{ei}^{ET}(\overline{c}, z) \le P_{max}^{ET},$$

$$\forall e \in ETS, i \in S, \overline{c} \in \overline{C}, z \in Z.$$
 (37)

## IV. GENERALIZED BENDERS DECOMPOSITION WITH SEQUENTIAL CONVEX PROGRAMMING (GBD-SCP)

The optimization problem in Section III is in a form of a Mixed Integer Nonlinear Problem (MINLP), which is known to be NP-hard in general [26], and there is no efficient way to solve this kind of problem optimally. Due to the nonconvexity of equation (5) and (8), the formulated problem is non-convex even with relaxation of the discrete variables. To solve the formulated problem, we first approximate equation (5) with a concave lower bound of the data rate function. Moreover, we reformulate constraint (26), add an additional and necessary constraint and relax it. Then, we use a sequential convex programming method with Generalized Bender Decomposition (GBD) algorithm [21] to find a solution for the optimization problem.

#### A. A Concave Lower Bound for the Data Rate Function

In this section, we find a concave lower bound for equation (5) since it is not a concave function. First, we rewrite equation (5) as follows:

$$R_{ij}(c,z) = W \log_2 \left( 1 + \frac{P_i^{tx}(c,z) \ G_{ij}^c}{\sum_{q \in S \setminus i} P_q^{tx}(c,z) \ G_{qj}^c + N_j} \right)$$

$$= W \log_2 \left( \sum_{q \in S} P_q^{tx}(c,z) \ G_{qj}^c + N_j \right)$$

$$- W \log_2 \left( \sum_{q \in S \setminus i} P_q^{tx}(c,z) \ G_{qj}^c + N_j \right)$$

$$\triangleq \hat{R}_{ij}(c,z)$$
(38)

To approximate equation (38) with a concave lower bound function, we approximate the second term, i.e.,  $\hat{R}_{ij}(c,z)$ , with a convex function. For the concave function  $\hat{R}_{ij}(c,z)$ , its first-order Taylor approximation around a point  $\tilde{P}_i(c,z)$  is a global overestimator [27]. Therefore,

$$\hat{R}_{ij}(c,z) \\
\leq W \log_2 \left( \sum_{q \in S \setminus i} \widetilde{P}_q(c,z) \ G_{qj}^c + N_j \right) \\
+ \sum_{q \in S \setminus i} \frac{W G_{qj}^c \log_2(e) \left[ P_i^{tx}(c,z) - \widetilde{P}_i(c,z) \right]}{\left[ \sum_{r \in S \setminus i} \widetilde{P}_r(c,z) \ G_{rj}^c + N_j \right]} \\
\triangleq \widetilde{R}_{ij}^{up}(c,z) \tag{39}$$

Hence, a concave lower bound function for equation (38) is given by

$$\overline{R}_{ij}(c,z) \triangleq W \log_2 \left( \sum_{q \in S} P_q^{tx}(c,z) \ G_{qj}^c + N_j \right) \\
- \widetilde{R}_{ij}^{up}(c,z).$$
(40)

#### B. Relaxing Energy Harvesting Function

The function  $E_i^H(z)$ , defined in (8), is nonconvex due to the noncovexity of the energy harvesting model described in equation (6). Similar to [25], we first introduce a slack variable  $\Delta_{ki}(c,z) = e^{[\tau P_{ki}^{ET}(c,z)G_{ki}^c]}$ . Then, we rewrite  $\eta_{ki}(c,z)$  as follows:

$$\eta_{ki}(c,z) = \left[\underbrace{\frac{P_{max}^{h}}{e^{-\tau\Gamma^{EH}+v}} \left(\frac{1+e^{-\tau\Gamma^{EH}+v}}{1+e^{v/\Delta_{ki}(c,z)}} - 1\right)}_{\triangleq \xi(\Delta(c,z))}\right]^{+} \tag{41}$$

From the equation above, we reformulate the function  $\xi(\Delta(c,z))$  as follows to make it a concave function [7]:

$$\xi(\Delta(c,z)) = \frac{P_{max}^{h} \left(1 + e^{-\tau \Gamma^{EH} + v}\right)}{e^{-\tau \Gamma^{EH} + v}} - \frac{P_{max}^{h}}{e^{-\tau \Gamma^{EH} + v}}$$

$$-\frac{P_{max}^{h}\left(1+e^{-\tau\Gamma^{EH}+v}\right)}{e^{-\tau\Gamma^{EH}+v}}\frac{e^{v}}{e^{v}+\Delta_{ki}(c,z)}$$
(42)

Finally, we relax  $\Delta_{ki}(c,z) = e^{[\tau P_{ki}^{ET}(c,z)G_{ki}^c]}$  into

$$\Delta_{ki}(c,z) \le e^{\left[\tau P_{ki}^{ET}(c,z)G_{ki}^c\right]} \tag{43}$$

It is shown in [7] that the solution of optimization problem is still optimal after dropping the operator  $[x]^+$  in equation (41) and relaxing  $\Delta_{ki}(c,z)$  as in (43). Accordingly, we can replace constraint (26) by

$$\sum_{z=1}^{|I|} E_i^{tx}(z) \le \sum_{z=1}^{|I|} \overline{E}_i^H(z), \quad \forall i \in S$$
 (44)

where  $\overline{E}_i^H(z)$  is defined as follows:

$$\overline{E}_{i}^{H}(z) = \sum_{c \in \overline{C}} \sum_{k \in ETS} T \, \xi(\Delta(c, z)). \tag{45}$$

Since  $\xi(\Delta(c,z))$  is concave function, and hence  $\overline{E}_i^H(z)$  is concave, the constraint (44) is convex.

From constraint (43), we have

$$\ln(\Delta_{ki}(c,z)) \le \tau P_{ki}^{ET}(c,z)G_{ki}^c \tag{46}$$

The constraint above is not convex. Therefore, we approximate  $\ln(\Delta_{ki}(c,z))$  using Taylor approximation around a point,  $\widetilde{\Delta}_{ki}(c,z)$ , as follows:

$$\ln\left(\widetilde{\Delta}_{ki}(c,z)\right) + \frac{\Delta_{ki}(c,z)}{\widetilde{\Delta}_{ki}(c,z)} - 1 \le \tau P_{ki}^{ET}(c,z)G_{ki}^{c}. \tag{47}$$

#### C. Generalized Benders Decomposition Steps

Generalized Benders Decomposition (GBD) [21] is a procedure used to solve non-convex MINLP problems. GBD method decomposes the non-convex MINLP into two subproblems, a master and a primal subproblems. The master subproblem is Mixed Integer Linear Program (MILP), whereas the primal subproblem is Non-linear Program (NLP). In each iteration of GBD algorithm, the upper and the lower bounds of the problem are given by solving the primal and the master problem, respectively,

The NLP subproblem in GBD algorithm corresponds to the original problem after fixing the binary variables. In addition to getting the upper bound after solving the NLP subproblem, we find the Lagrange multipliers associated with the constraints of the NLP subproblem. From non-linear duality theory, the Lagrange multipliers of the primal problem are used in the master problem to find the lower bound. The solution of the binary variables given by the master problem are used by the primal subproblem in the next iteration, and the algorithm iterates until the algorithm converges.

In the following, we describe four steps to solve the optimization problem iteratively using GBD with Sequential Convex Programming (SCP). These steps are: 1) Initialization; 2) Solving the primal problem; 3) Solving the feasibility problem; and 4) Solving the master Problem. A complete overview of the algorithm is shown in Algorithm 1.

*Note:* In Algorithm 1, we use + superscript on the binary variables to indicate their solution after being fixed. Moreover, the continuous variables with (k) and (l) superscripts indicate their values after the primal and feasibility problems being solved feasibly in the  $k^{th}$  and  $l^{th}$  times, respectively.

- 1) Initialization: We find initial values for all binary variable,  $\widetilde{P}_i(c,z)$  and  $\widetilde{\Delta}_{ki}(c,z)$ , then we set  $X_i^+(c,z)=X_i(c,z),\ X_{ij}^+(c,z)=X_{ij}(c,z),\ H_i^+(\overline{c},z)=H_i(\overline{c},z)$  and  $H_{ei}^+(\overline{c},z)=H_{ei}(\overline{c},z),\ \forall i\in S,\ j\in \overline{S},\ e\in ETS,\ c\in C,\ \overline{c}\in \overline{C},\ z\in Z.$  Moreover, we set the counter, k and l, to 1.
- 2) Primal Problem: After fixing all binary variables, the primal problem transforms the MINLP problem into an NLP problem. We use a concave lower bound function  $\overline{R}_{ij}(c,z)$  in equation (40) to approximate the data rate function in equation (38) to preserve the convexity of the primal problem in GBD algorithm. Moreover, we replace constraint (26) by constraint (44) and (47) to approximate the original optimization problem by a convex approximation. Accordingly, we formulate the primal problem as a convex NLP program as follows:

#### P2.1: Minimize:

$$\pi = \sum_{e \in ETS} \sum_{i \in S} \sum_{c \in \overline{C}} \sum_{z=1}^{|I|} P_{ei}^{ET}(c, z) \ T$$
 (48)

#### Subject to:

Constraints (19-24), (29-31), (35-37), (44) and (47).

$$X_{ij}^{+}(c,z) - \sum_{y=1}^{|d|} f_{ij}^{y}(c,z) \le 0,$$

$$\forall i \in S, j \in \overline{S}, c \in C, z \in Z.$$

$$\frac{f_{ij}^{y}(c,z)}{v} - X_{ij}^{+}(c,z) \le 0,$$
(49)

$$\forall i \in S, j \in \overline{S}, c \in C, y \in d, z \in Z.$$
 (50)

$$P_i^{tx}(c,z) - P_{max}^{tx} X_i^+(c,z) \le 0,$$

$$\forall i \in S, c \in C, z \in Z.$$

$$P_{ei}^{ET}(c, z) - P_{max}^{ET} H_i^+(c, z) \le 0,$$
(51)

$$F_{ei}$$
  $(c, z) - F_{max} H_i$   $(c, z) \le 0$ ,  
 $\forall e \in ETS, i \in S, c \in \overline{C}, z \in Z.$  (52)

$$f_{ij}^{y}(c,z) - X_{ij}^{+}(c,z) \overline{R}_{ij}(c,z) T \leq 0,$$

$$\forall i \in S, j \in \overline{S}, y \in d, c \in C, z \in Z.$$
 (53)

$$X_i^+(c,z) - \frac{BL_i(z)}{BL^{min}} \le 0, \forall i \in S, c \in C, z \in Z. \quad (54)$$

$$\Gamma^{M2M} X_{ij}^{+}(c,z) \left[ \sum_{q \in S \setminus i} P_q^{tx}(c,z) G_{qj}^c + \alpha_{ij} \right]$$

$$-P_i^{tx}(c,z) G_{ij}^c \le 0$$

$$\forall i \in S, j \in \overline{S}, c \in C, z \in Z.$$

$$(55)$$

$$\Gamma^{EH} H_{ei}^+(c,z) - P_{ei}^{ET}(c,z) G_{ei}^c \le 0,$$

$$\forall e \in ETS, i \in S, c \in \overline{C}, z \in Z.$$
 (56)

$$1 \le \Delta_{ei}(c, z), \forall e \in ETS, i \in S, c \in \overline{C}, z \in Z.$$
 (57)

After finding an optimal solution for P2.1, we need to derive the Lagrange multipliers associated with the constraints (49–56). The master problem uses these multipliers

to find solutions for the binary variables. Let  $\Phi^{(k)}$  be the set of Lagrange multipliers associated with P2.1, i.e.,  $\Phi^{(k)} = \{\lambda^k(i,j,c,z), \ \Lambda^k(i,j,y,c,z), \ \omega^k(i,c,z), \ \Omega^k(e,i,\overline{c},z), \ \theta^k(i,j,y,c,z), \ \Theta^k(i,c,z), \zeta^k(i,j,c,z), \psi^k(e,i,\overline{c},z)\}, \ \forall i \in S, \ \forall j \in \overline{S}, \ \forall e \in ETS, \ \forall y \in d, \ \forall c \in C, \ z \in Z, \ 1 \leq n \leq k.$  The set members of  $\Phi^{(k)}$  are associated with lagrange multipliers of the constraints (49-56), respectively.

3) Feasibility Problem: When the primal problem solution is not feasible, we solve the feasibility problem to use its Lagrange multipliers in solving the master problem. The feasibility problem is similar to the primal problem except that we introduce some variables that serve as upper bounds for all constraints, and the objective function is to minimize the sum of these variables in order to minimize the sum of the constraints violations. Therefore, the feasibility problem can be formulated as follows:

#### P2.2: Minimize:

$$\sum_{z=1}^{|I|} \sum_{\forall i \in S} \left( \sum_{\forall c \in C} (u_3(i, c, z) + u_6(i, c, z)) \right)$$

$$+ \sum_{\forall j \in \overline{S}} \left( [u_1(i,j,c,z) + u_7(i,j,c,z)] + \sum_{y=1}^{|d|} [u_2(i,j,y,c,z) + u_5(i,j,y,c,z)] \right)$$

$$+ \sum_{\forall e \in ETS} \sum_{\forall \overline{c} \in \overline{C}} [u_4(e,i,\overline{c},z) + u_8(e,i,\overline{c},z)] \right)$$
(60)

#### Subject to:

Constraints (19-24), (29-31), (35-37), (44), (47) and (57).

$$X_{ij}^{+}(c,z) - \sum_{y=1}^{|d|} f_{ij}^{y}(c,z) \le u_{1}(i,j,c,z)$$

$$\forall i \in S, j \in \overline{S}, c \in C, z \in Z.$$

$$f_{ij}^{y}(c,z) - X_{ij}^{+}(c,z) \le u_{2}(i,j,y,c,z)$$

$$\forall i \in S, j \in \overline{S}, c \in C, y \in d, z \in Z.$$

$$(61)$$

$$\mathcal{L}\left(X_{i}(c,z), X_{ij}(c,z), H_{i}(\overline{c},z), H_{ei}(\overline{c},z), f_{ij}^{y(k)}(c,z), P_{i}^{tx(k)}(c,z), P_{ei}^{ET(k)}(\overline{c},z)\right)$$

$$= \sum_{\widetilde{e} \in ETS} \sum_{\widetilde{i} \in S} \sum_{\widetilde{c} \in C} \sum_{\widetilde{z}=1}^{|I|} P_{\widetilde{e}\widetilde{i}}^{ET(k)}(\widetilde{c},\widetilde{z}) T$$

$$+ \lambda^{k}(i,j,c,z) \left(X_{ij}(c,z) - \sum_{q=1}^{|d|} f_{ij}^{q(k)}(c,z)\right) + \Lambda^{k}(i,j,y,c,z) \left(\frac{f_{ij}^{y(k)}(c,z)}{v} - X_{ij}(c,z)\right)$$

$$+ \Theta^{k}(i,z) \left(X_{i}(c,z) - \frac{BL_{i}(z)^{(k)}}{BL^{min}}\right) + \Omega^{k}(e,i,\overline{c},z) \left(P_{ei}^{ET(k)}(\overline{c},z) - P_{max}^{ET} H_{ei}(\overline{c},z)\right)$$

$$+ \theta^{k}(i,j,y,c,z) \left(f_{ij}^{y(k)}(c,z) - X_{ij}(c,z) \overline{R}_{ij}^{(k)}(c,z) T\right)$$

$$+ \omega^{k}(i,c,z) \left(P_{i}^{tx(k)}(c,z) - P_{max}^{tx} X_{i}(c,z)\right) + \psi^{k}(e,i,\overline{c},z) \left(\Gamma^{EH} H_{ei}(\overline{c},z) - P_{ei}^{ET(k)}(\overline{c},z) G_{ei}^{c}\right)$$

$$+ \zeta^{k}(i,j,c,z) \left(\Gamma X_{ij}(c,z) \left[\sum_{q \in S \setminus i} P_{q}^{tx(k)}(c,z) G_{qj}^{c} + \alpha_{ij}\right] - P_{i}^{tx(k)}(c,z) G_{ij}^{c}\right)$$
(58)

$$\hat{\mathcal{L}}\left(X_{i}(c,z), X_{ij}(c,z), H_{i}(\overline{c},z), H_{ei}(\overline{c},z), f_{ij}^{y(l)}(c,z), P_{i}^{tx(l)}(c,z), P_{ei}^{ET(l)}(\overline{c},z)\right) \\
= \hat{\lambda}^{l}(i,j,c,z) \left(X_{ij}(c,z) - \sum_{q=1}^{|d|} f_{ij}^{q(l)}(c,z)\right) + \hat{\Lambda}^{l}(i,j,y,c,z) \left(\frac{f_{ij}^{y(l)}(c,z)}{v} - X_{ij}(c,z)\right) \\
+ \hat{\Theta}^{l}(i,c,z) \left(X_{i}(c,z) - \frac{BL_{i}(z)^{(l)}}{BL^{min}}\right) + \hat{\Omega}^{l}(e,i,\overline{c},z) \left(P_{ei}^{ET(l)}(\overline{c},z) - P_{max}^{ET} H_{ei}(\overline{c},z)\right) \\
+ \hat{\theta}^{l}(i,j,y,c,z) \left(f_{ij}^{y(l)}(c,z) - X_{ij}(c,z) \overline{R}_{ij}^{(l)}(c,z) T\right) + \hat{\psi}^{l}(e,i,\overline{c},z) \left(\Gamma^{EH} H_{ei}(\overline{c},z) - P_{ei}^{ET(l)}(\overline{c},z) G_{ei}^{c}\right) \\
\hat{\omega}^{l}(i,c,z) \left(P_{i}^{tx(l)}(c,z) - P_{max}^{tx} X_{i}(c,z) + \hat{\zeta}^{l}(i,j,c,z) \left(\Gamma X_{ij}(c,z) \overline{R}_{q}^{tx(l)}(c,z) G_{qj}^{c} + \alpha_{ij}\right] - P_{i}^{tx(l)}(c,z) G_{ij}^{c}\right) \right) \tag{59}$$

$$\begin{split} P_{i}^{tx}(c,z) - P_{max}^{tx}X_{i}^{+}(c,z) &\leq u_{3}(i,c,z), \\ \forall i \in S, c \in C, z \in Z. \\ P_{ei}^{ET}(c,z) - P_{max}^{ET}H_{ei}^{+}(c,z) &\leq u_{4}(e,i,c,z) \\ \forall e \in ETS, i \in S, c \in \overline{C}, z \in Z. \\ \forall i \in S, j \in \overline{S}, i \in S, c \in \overline{C}, z \in Z. \\ \forall i \in S, j \in \overline{S}, j \in J, j \in J,$$

Let  $\hat{\Phi}^{(l)}$  be the set of Lagrange multipliers associated with the feasibility problem P2.3, i.e.,  $\Phi^{(l)} = \{\hat{\lambda}^l(i,j,c,z), \hat{\Lambda}^l(i,j,y,c,z), \hat{\omega}^l(i,c,z), \hat{\Omega}^l(e,i,\overline{c},z), \hat{\theta}^l(i,j,y,c,z), \hat{\Theta}^l(i,c,z), \hat{\zeta}^l(i,j,c,z), \hat{\psi}^l(e,i,\overline{c},z)\}, \ \forall i \in S, \ j \in \overline{S}, \ e \in ETS, \ y \in d, \ c \in C, \ \overline{c} \in \overline{C}, \ z \in Z, \ 1 \leq n \leq k.$  The set members of  $\hat{\Phi}^{(l)}$  are associated with lagrange multipliers of the constraints (61-68), respectively.

4) Master Problem: The master problem uses support functions in the model to provide a lower bound solution. These support functions are given in equations (58) and (59), shown at the bottom of the previous page. Hence, the master problem can be formulated as an MILP as follows:

$$P2.3: Minimize: \mu$$
 (70)

#### Subject to:

Constraints (9), (12-15), (28), (34).

$$\mathcal{L}\left(X_{i}(c,z), X_{ij}(c,z), H_{i}(\overline{c},z), H_{ei}(\overline{c},z), f_{ij}^{y(n)}(c,z), P_{i}^{tx(n)}(c,z), P_{ei}^{ET(n)}(\overline{c},z)\right) \leq \mu$$

$$\forall i \in S, j \in \overline{S}, e \in ETS, y \in d,$$

$$c \in C, \overline{c} \in \overline{C}, z \in Z, 1 \leq n \leq k. \tag{71}$$

$$\hat{\mathcal{L}}\left(X_{i}(c,z), X_{ij}(c,z), H_{i}(\overline{c},z), H_{ei}(\overline{c},z), f_{ij}^{y(q)}(c,z), P_{i}^{tx(q)}(c,z), P_{ei}^{ET(q)}(\overline{c},z)\right) \leq 0$$

$$\forall i \in S, j \in \overline{S}, e \in ETS, y \in d,$$

$$c \in C, \overline{c} \in \overline{C}, z \in Z, 1 \leq q \leq l. \tag{72}$$

### D. GBD-SC Algorithm

Due to the non-convexity of equation (5), we substitute it with an approximate function defined by equation (40).

Moreover, constraint (26) is non-convex. Therefore, we provide an approximation for the problem by replacing (26) by constraint (44) and adding constraint (47). Given an initial point value for  $\widetilde{P}_i(c,z)$  and  $\widetilde{\Delta}_{ki}(c,z)$ , we embed SCP within GBD algorithm to solve the primal problem successively in order to get a better approximation for the original problem.

Initial values for  $\widetilde{P}_i(c,z)$  and  $\widetilde{\Delta}_{ki}(c,z)$  can be set to  $P^{tx}_{max}(c,z)$  and  $e^{[\tau P^{ET}_{max}(c,z)G^c_{ki}]}$ , respectively. Without loss of generality, we assume that finding feasible initial values for the binary variables is possible. However, when the initial values of the binary variables lead to infeasible solution for the primal problem, feasibility problem can be used to get the Lagrange multipliers to be used in solving the master problem then continue the iteration of GBD-CS Algorithm. One way to get possible feasible initial values for the binary variables is to solve an optimization problem that minimizes the sum of all binary variables subject to all linear constraints in P1 associated with the flow,  $f_{ij}^{y}(c,z)$ , and the binary variables.

Algorithm 1 shows the required steps to solve our problem using GBD and SCP. In steps 1-3, we find initial values for the binary variables,  $\widetilde{P}_i(c,z)$  and  $\widetilde{\Delta}_{ki}(c,z)$ , then we solve the primal problem using SCP algorithm to get the upper bound and the initial values for the multipliers. Then, we define the fixed values for the continuous variables to be used by the master problem. We assume that we can get a feasible solution for the primal problem using the selected initial values. However, it is possible to solve the feasibly problem if the solution of the primal problem is infeasible to find the required Lagrange multipliers for the master problem. In step 4-9, we solve the master problem and find the lower bound. The algorithm terminates if the difference between the upper and the lower bounds is less than a threshold  $\epsilon$ .

In steps 10-18, we solve the primal problem again after fixing the binary variables with their new values, and we get the upper bound and the multipliers if the solution is feasible. The algorithm terminates if the gap between the upper and the lower bounds is less than a threshold  $\epsilon$ . If the solution is not feasible, we solve the feasibility problem to get the Lagrange multipliers as shown in steps 19-23. Then, the algorithm iterates until the target gap between the upper and the lower bounds is achieved.

It is shown in Algorithm 2 that SCP terminates when the solution does not change or when the maximum number of iterations is reached. Moreover the set of all binary variables in the optimization problem is finite. Therefore, Algorithm 1 terminates in a finite number of steps for any positive convergence tolerance parameter,  $\epsilon$ , as shown in [21].

## V. CONSTRAINTS DECOMPOSITION WITH BINARY VARIABLES RELAXATION (CDR)

In Section IV, we use a convex approximation for the non-convex data rate function. Then, we decompose the problem into two subproblems: 1) Convex NLP and 2) MILP using GBD and SCP. Although this method facilitates finding a solution for the original optimization problem, the problem is still NP-Hard due to the binary variables in the master problem. Therefore, in this section we propose another method for

**Algorithm 1:** Generalized Benders Decomposition With Sequential Convex Programming (GBD-SCP)

```
1 Select initial fixed values for X_i(c, z), X_{ij}(c, z),
     H_i(\overline{c}, z), H_{ei}(\overline{c}, z), P_i(c, z) \text{ and } \Delta_{ei}(c, z), \forall i \in S,
    j \in \overline{S}, e \in ETS, c \in C, \overline{c} \in \overline{C}, z \in Z, solve problem
    P2.1 using Algorithm 2, and let its solution and the
    corresponding Lagrange multipliers set be \pi^{(1)} and \Phi^{(1)},
    respectively.
2 Set k = 1, l = 0, UB = \pi^{(1)}.
3 Set, f_{ii}^{y(1)}(c,z) = f_{ii}^{y*}(c,z), \widetilde{P}_i(c,z) = P_i^{tx*}(c,z),
\widetilde{\Delta}_{ei}(c,z) = \Delta_{ei}(c,z), \ P_i^{tx(1)}(c,z) = P_i^{tx*}(c,z), \\ P_{ei}^{ET(1)}(\overline{c},z) = P_{ei}^{ET*}(\overline{c},z). \\ \text{4 Solve problem P2.2.}
5 Let the solution of P2.2 be \mu^*, and set LB = \mu^*.
 6 if (UB - LB) < \epsilon then
7
           Terminate.
8 else
         X_{i}^{+}(c,z) = X_{i}^{*}(c,z), \ X_{ij}^{+}(c,z) = X_{ij}^{*}(c,z), 
 H_{i}^{+}(\overline{c},z) = H_{i}^{*}(\overline{c},z), \ H_{ei}^{+}(\overline{c},z) = H_{ei}^{*}(\overline{c},z), 
 \widetilde{P}_{i}(c,z) = P_{i}^{tx*}(c,z) \ X_{i}^{*}(c,z). 
10 Solve problem P2.1 using Algorithm 2.
11 if (The solution of Algorithm 2, \pi^{(k)}, is feasible and
     optimal multipliers are found) then
            UB = \min(UB, \pi^{(k)}).
12
           if (UB - LB) < \epsilon then
13
                 Terminate.
14
15
           else
                  k = k + 1.
16
                 Let the corresponding Lagrange multipliers set be
17
                 f_{ij}^{y(k)}(c,z) = f_{ij}^{y*}(c,z), \ \widetilde{P}_i(c,z) = P_i^{tx*}(c,z),
18
                \begin{split} &\overset{ij}{\Delta}_{ei}(c,z) = \Delta_{ei}(c,z), \\ &P_i^{tx(k)}(c,z) = P_i^{tx*}(c,z), \\ &P_{ei}^{ET(k)}(\overline{c},z) = P_{ei}^{ET*}(\overline{c},z). \end{split}
19 else
           Solve the feasibility problem, P2.3.
20
           Find the corresponding Lagrange multipliers set, \hat{\Phi}^{(l)}.
21
          f_{ij}^{y(l)}(c,z) = f_{ij}^{y*}(c,z), \ P_i^{tx(l)}(c,z) = P_i^{tx*}(c,z), 
P_{ei}^{ET(l)}(\overline{c},z) = P_{ei}^{ET*}(\overline{c},z).
23
```

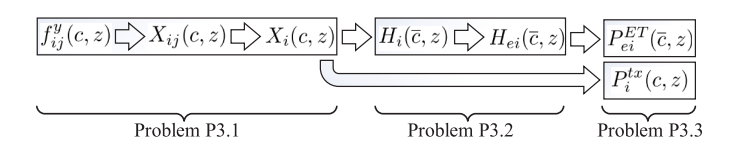


Fig. 2. Decision variables dependencies.

24 Go to step 4.

solving the original optimization problem based on constraints decomposition and binary variables relaxation.

Fig. 2 shows how the decision variables depend on each other. To get an advantage of this property, we decompose the problem into three subproblems accordingly. Due to

**Algorithm 2:** Sequential Convex Programming (SCP)

```
1 r = 1, \Pi^{(0)} = \infty
2 while (r \neq Max iterations) do
        Solve the optimization problem, and let its solution
        if (The solution is feasible) then
4
             if (\Pi^{(r-1)} - \Pi^{(r)} > \delta) then
5
                  \widetilde{P}_i(c,z) = P_i^{tx*}(c,z).
6
                  \widetilde{\Delta}_{ei}(c,z) = \Delta_{ei}(c,z).
7
8
9
                  \pi^{(k)} = \Pi^{(r)}.
10
                  Terminate.
11
        else
12
13
             Terminate.
```

constraint (9) and relaxation of the binary variables, we decompose the binary variables of data transmission (i.e.,  $X_i(c,z)$  and  $X_{ij}(c,z)$ ) and the binary variables for energy harvesting (i.e.,  $H_i(\overline{c},z)$ ) and  $H_{ei}(\overline{c},z)$ ) into two problems. Hence, We find solutions for the flow  $f_{ij}^y(c,z)$ ,  $X_i(c,z)$  and  $X_{ij}(c,z)$  in problem P3.1, then we round the relaxed binary variables up to 1. Then, we solve problem P3.2 to get solutions for  $H_i(\overline{c},z)$  and  $H_{ei}(\overline{c},z)$ . Note that the solution of the relaxed binary variable can only be zero or a positive number less than or equals one. Hence, we round the positive solution of each relaxed binary variable up to 1. Finally, we can solve problem P3.2 where  $P_i^{tx}(c,z)$  and  $P_{ei}^{ET}(\overline{c},z)$  depend on the found solution of the binary variables. In the following, we formulate these subproblems and describe the proposed algorithm for solving the optimization problem.

*Note:* In CDR algorithm, we use + superscript on the binary variables to indicate their solution after being fixed. Moreover, the continuous variables with (k) superscripts indicate their values after being solved in the  $k^{th}$  iteration of CDR algorithm.

#### A. Problem P3.1

The goal of solving this problem is to find solutions for the relaxed  $X_i(c,z)$  and  $X_{ij}(c,z)$  variables. From Fig. 2, we can find solutions for  $f^y_{ij}(c,z)$  variables by solving the multicast flow conservation constraints, then we can decide the values of  $X_i(c,z)$  and  $X_{ij}(c,z)$  accordingly. To explore a variety of different solutions for the decision variables, we solve problem P3.1 such that we get different solutions for the relaxed binary variables in each run of P3.1 problem.

We define a set,  $\rho$ , where it contains initially all  $X_{ij}(c,z)$  variables. After solving P3.1 problem, we remove each  $X_{ij}(c,z)$  variable from set  $\rho$  if its solution is positive. From constraint (74), we can get different solution for  $X_{ij}(c,z)$  variables after each run of problem P3.1 in CDR algorithm. Different solutions for  $X_{ij}(c,z)$  variables may lead to finding different solutions for  $H_{ei}(\overline{c},z)$  variables in problem P3.2, and hence, different solutions for  $P_{ei}^{tx}(c,z)$  and  $P_{ei}^{ET}(\overline{c},z)$  in

4

5

7

8

11

12

14

15

16

17

18

problem P3.3. Accordingly, We can formulate P3.1 problem as follows:

**P3.1 : Minimize:** 
$$\sum_{z=1}^{|I|} \sum_{c \in C} \sum_{i \in S} \sum_{j \in \overline{S}} \sum_{y \in d} f_{ij}^{y}(c, z)$$
 (73)

#### Subject to:

Constraints (10-13), (19-23) and (35).

$$\sum_{X_{ij}(c,z)\in\rho} X_{ij}(c,z) > 0. \tag{74}$$

$$0 \le X_i(c, z) \le 1, \ \forall i \in S, c \in C, z \in Z. \tag{75}$$

$$0 \le X_{ij}(c,z) \le 1, \forall i \in S, j \in \overline{S}, c \in C, z \in Z.$$
 (76)

#### B. Problem P3.2

After finding solutions for  $X_i(c, z)$  and  $X_{ij}(c, z)$  in P3.1, we round them up to 1 and fix them in addition to fixing  $f_{ij}^{y}(c,z)$ . Then, we solve P3.2 in order to find solutions for  $H_i(\overline{c}, z)$  and  $H_{ei}(\overline{c}, z)$ . Hence, we can formulate problem P3.2 as follows:

**P3.2 : Maximize:** 
$$\sum_{e \in ETS} \sum_{i \in S} \sum_{c \in \overline{C}} \sum_{z=1}^{|I|} P_{ei}^{ET}(c,z) \ T \ (77)$$

#### Subject to:

Constraints (14-15), (24), (25), (27-31), (36-37), (44), (47), (51), (54-55), and (57)

$$\sum_{c \in C} \left[ X_i^+(c,z) + \sum_{\forall q \in \overline{S}} X_{qi}^+(c,z) \right] + \sum_{c \in \overline{C}} H_i(c,z) \le 1,$$

$$\forall i \in S, z \in Z. \tag{78}$$

$$f_{ij}^{y +}(c,z) - X_{ij}^+(c,z) \, \overline{R}_{ij}(c,z) \, T \le 0,$$

$$\forall i \in S, j \in \overline{S}, y \in d, c \in C, z \in Z. \tag{79}$$

$$0 \le H_i(c,z) \le 1, \, \forall i \in S, c \in \overline{C}, z \in Z. \tag{80}$$

$$0 \le H_{ei}(c,z) \le 1, \, \forall i \in S, e \in ETS, c \in \overline{C}, z \in Z. \tag{81}$$

#### C. Problem P3.3

In problem P3.1 and P3.2, we find solutions for the relaxed binary variables. Therefore, we can formulate P3.3 as a convex NLP to get a solution for power allocation subproblem as follows:

**P3.3 : Minimize:** 
$$\sum_{i \in S} \sum_{e \in ETS} \sum_{i \in S} \sum_{c \in \overline{C}} \sum_{z=1}^{|I|} P_{ei}^{ET}(c, z) T$$
 (82)

Constraints (19-24), (29-31), (35-37), (44), (47), (49-56) and (57).

#### D. CDR Algorithm

The CDR algorithm is described in Algorithm 3. In this algorithm, we solve problem P3.1, P3.2 and P3.3 iteratively after decomposing the original optimization problem. Moreover, we employ Algorithm 2 to find approximation for the non-convex data rate function. In steps 1-2, Algorithm 3

Algorithm 3: Constraints Decomposition With SCP and Binary Variable Relaxation (CDR)

```
1 Set k = 1. \Pi = \infty and Count = 0.
2 \rho = \{X_{ij}(c,z)\}, \forall i \in S, \forall j \in \overline{S}, \forall c \in C, z \in Z.
3 while (Count \neq Termination Threshold and \rho \neq \{\emptyset\})
    do
          Solve problem P3.1.
          if (The solution of P3.1 is feasible) then
                 Round the solutions of X_i(c,z) and X_{ij}(c,z) up
                to 1, i.e., X_i^+(c,z) = \lceil X_i^*(c,z) \rceil and X_{ij}^+(c,z) = \lceil X_{ij}^*(c,z) \rceil, \forall i \in S, \ \forall j \in \overline{S}, \ \forall c \in C, \ z \in Z.
                Remove X_{ij}(c,z) from \rho \ \forall \ X_{ij}^+(c,z) = 1.
                Solve problem P3.2.
                if (The solution of P3.2 is feasible) then
                      Set \widetilde{P}_i(c,z) = P_i^{tx*}(c,z) and
                      \widetilde{\Delta}_{ei}(c,z) = \Delta_{ei}(c,z), \forall i \in S, e \in ETS,
                       \forall c \in C, z \in Z.
                       Round the solutions of H_i(\overline{c}, z) and H_{ei}(\overline{c}, z)
                      up to 1, i.e., H_i^+(\overline{c},z) = \lceil H_i^*(\overline{c},z) \rceil, H_{ei}^+(\overline{c},z) = \lceil H_{ei}^*(\overline{c},z) \rceil, \forall i \in S, e \in ETS, \overline{c} \in C, z \in Z.
                      Solve P3.3 using Algorithm 2, and let the
                      solution be \pi^{(k)}.
                      if (The solution of Algorithm 2 is feasible)
                      then
                             if (\pi^{(k)} = \Pi) then
                               Count = Count + 1.
                             \begin{array}{ll} \mbox{if} & \left( \ \pi^{(k)} < \Pi \ \right) \ \mbox{then} \\ \mid & \Pi = \pi^{(k)}. \end{array}
                                   Count = 0.
          k = k + 1.
```

initialize some counters and parameters to be used by the algorithm. Moreover, Algorithm 3 initialized the set  $\rho$  to contain all binary variables  $X_{ij}(c,z)$ . In steps 4-7, we solve problem P3.1, round the relaxed variables up to 1 and remove them from  $\rho$  if they are positive. In steps 8-11, we solve P3.2 and round the solution of the relaxed binary variables up to one. Then we solve the problem of minimizing total transmitted energy in step 12 using Algorithm 2. Steps 13-18 lead to termination of Algorithm 3 when the solution of the algorithm is repeated in the recent iterations for a number of times equals Count. Moreover, Algorithm 3 will terminate when the set  $\rho$ becomes empty.

Theorem 1: Given a finite number of users, channels and time slots, CDR algorithm converges in a finite number of steps.

*Proof:* In P3.1, constraint (74) ensures that at least one new variable  $X_{ij}(c,z) \in \rho$  is greater than zero in each iteration of Algorithm 3. Moreover, Algorithm 3 removes all positive variables  $X_{ij}(c,z)$  from  $\rho$  during each iteration. It

D	Value		
Parameter	value	Parameter	Value
$PL_c$	10-2	v	0.29
$PL_e$	2	$P_{max}^{tx}$	250 mW
$\phi$	15°	$P_{max}^{ET}$	20 W
$\overline{\phi}$	20°	$P_{max}^{ET}$ $P^{BS}$	20 W
W	6 MHz	T	1 sec
$N_0$	-174 dbm/Hz	q	1 Mb
$\Gamma^{EH}$	0.064 mW	$BL^{min}$	10 mAh
$\Gamma^{M2M}$	10	$BL_i^{init}$	300 mAh
$\Gamma^{cell}$	10	$BL_i^{max}$	500 mAh
τ	274	$\epsilon$	0.01
$P_{max}^h$	4.927 mW	δ	0.01

TABLE II SIMULATION PARAMETERS

is shown in Algorithm 3 that one of the termination conditions is when the set  $\rho$  is empty. Hence, the maximum number of iterations for Algorithm 3 is reached when one variable  $X_{ij}(c,z) \in \rho$  is removed from  $\rho$  in each iteration. In other words, the number of iterations for CDR algorithm is upper bounded by the maximum cardinality of set  $\rho$ , which is  $|S| \times |\overline{S}| \times |C| \times |Z|$ .

#### VI. SIMULATION RESULTS

In this section, we study the problem of minimizing the total transferred energy to support M2M multicast service for IoT devices in cellular networks. We use General Algebraic Modeling System (GAMS) [28] with SCIP solver [29] to solve the original optimization problem, P1, optimally. It is shown in [29] that SCIP uses a spatial branch-and-bound algorithm to solve convex and non-convex MINLP problem to achieve global optimality. Moreover, we use CPLEX [30] and Interior Point Optimizer (IPOPT) [31] under GAMS to solve MILP and NLP problems, respectively.

We consider in the simulation two network sizes: 1) Small networks and 2) Larger networks. The network size is represented here by the number of devices and ETs. Unless the network parameters are specified otherwise, the small network consists of 1 BS, 1 ET, 8 cellular devices and 5 M2M devices. On the other hand, the large network consists of 1 BS, 4 ETs, 8 cellular devices and 10 M2M devices.

Due to the difficulty of finding the optimal solution when the network size is large, we compare the optimal solution with GBD-SCP and CDR algorithm using small networks. For the other performance comparisons in this section, we use the larger network. Similar to [12], we assume that the ETs are distributed within 100 meter of the BS. The distribution of the multipath fading and the shadowing are exponential with unit mean and log-normal with standard deviation of 8 dB, respectively. The rest of the simulation parameters are shown in Table II.

Fig. 3 shows a comparison between the optimal solution and the solutions given by GBD-SCP and CDR algorithms. As the number of iterations for CDR algorithm increases, the performance improves significantly until it stabilizes when it reaches around the  $6^{th}$  iteration. Both GBD-SCP and CDR achieve performance close to the optimal although GBD-SCP outperforms CDR.

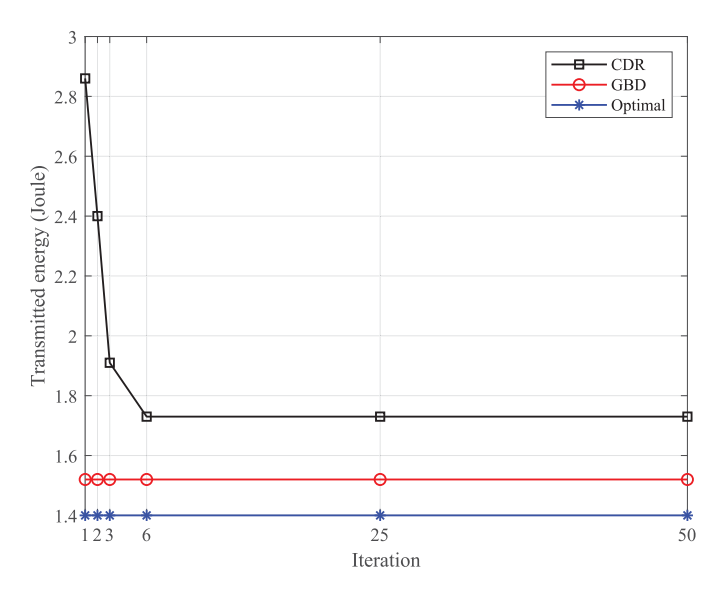


Fig. 3. A comparison between the optimal solution and the solutions given by GBD-SCP and CDR algorithms.

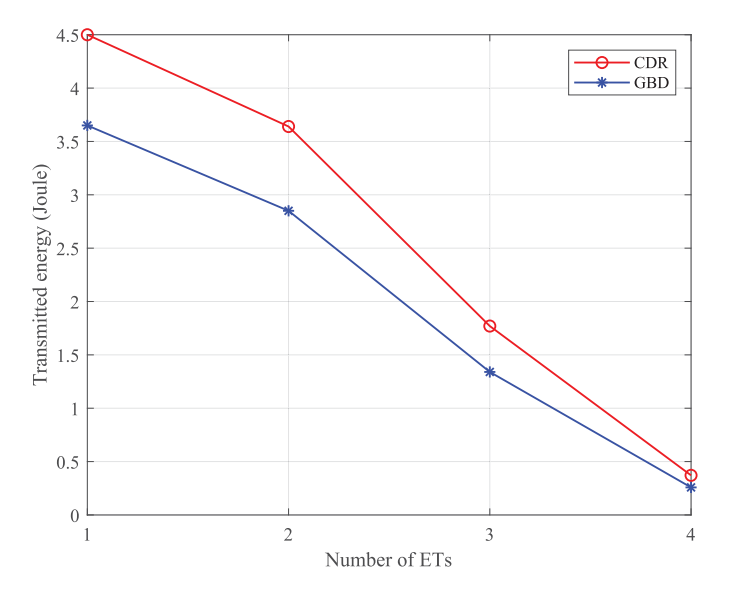


Fig. 4. Transmitted energy vs number of ETs.

Fig. 4 shows the effect of increasing the number of ETs on the total transmitted energy when the network is larger and CDR iterations are 10. The performance difference between GBD-SCP and CDR algorithms decreases by increasing the number of ETs. Moreover, the total required energy to be transferred decreases as the number of ETs increases, as shown in Fig. 4. The reason for this trend is that increasing the number of ETs increases the chances for the M2M devices to receive energy from closer ETs and over channels with better conditions. Hence, less energy can be transferred while supporting the same energy demands for the M2M devices.

Table III shows the computation times when the problem is solved optimally and when GBD-SCP and CDR are used. We select the number of iterations for CDR algorithm to be 10 since its performance is close to the optimal and the performance of GBD-SCP algorithm when the network size is small and large, respectively. It is shown that finding the

TABLE III COMPUTATION TIME (SECONDS)

	Small Network	Large Network
Optimal	129	N/A
GBD	61	73
CDR	13	16

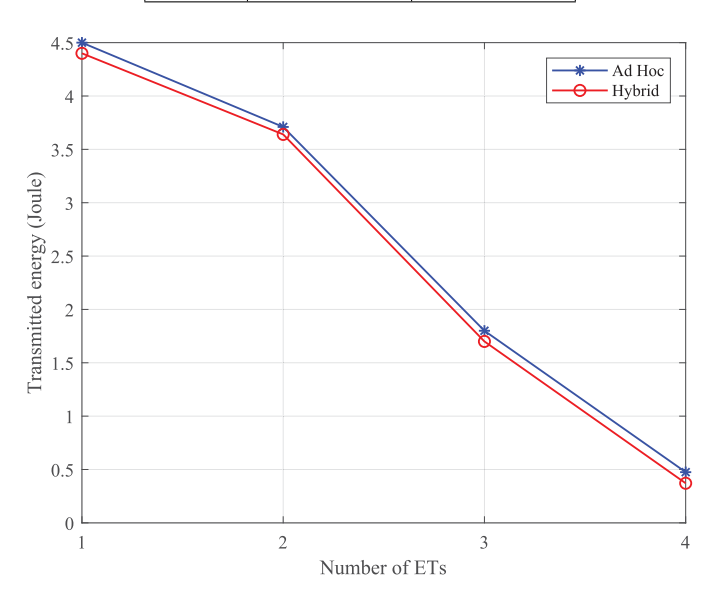


Fig. 5. Transmitted energy vs. number of ETS when the network architecture is ad hoc and hybrid.

optimal solution when the network size is small requires long computation time whereas it cannot be found efficiently when the network is large. Moreover, Table III indicates that GBD-SCP and CDR algorithms reduce the computation time significantly when the network is small, and they can find solutions when the network is large. CDR algorithm outperforms GBD-SCP when the network size is small and large. GBD-SCP algorithm performance is significantly influenced by solving the MILP problem, which consists of binary variable. However, CDR algorithm solves the problem while relaxing the binary variables, and this contributes to reducing the computation time.

To study the effect of the network architecture on the total transmitted energy, we consider hybrid and ad hoc networks architectures. A hybrid network is similar to the network architecture shown in Fig. 1 where the multicast message can be transmitted using M2M communication links and the cellular downlink from the BS to the M2M devices. On the other hand, the multicast message is transmitted using only M2M communication in ad hoc network architecture without help from the BS.

Fig. 5 and Fig. 6 show the effect of the network architecture on the transmitted energy. Since only the transmitting M2M devices are compensated by energy for their consumed energy to transmit a multicast message, the BS can help in reducing the total consumed energy by M2M devices by forwarding the multicast message to the destinations. Hence, the total transmitted energy can be reduced by using the hybrid network architecture as shown in Fig. 5 and Fig. 6. On the other hand, increasing the number of destinations when the

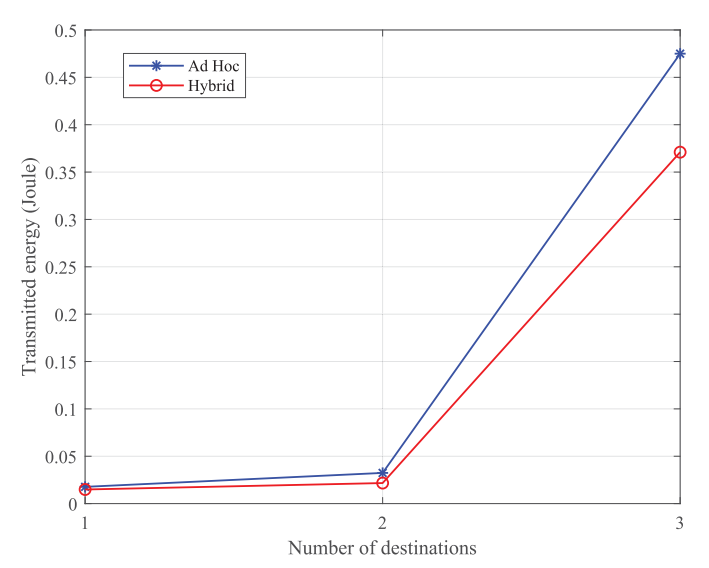


Fig. 6. Transmitted energy vs. number multicast destination when the network architecture is ad hoc and hybrid.

network is ad hoc generally results in more M2M communications, and hence, more energy consumption by the M2M devices. Therefore, the ETs transmit more energy as the number of destinations increases in the ad hoc network architecture as shown in Fig. 6.

#### VII. CONCLUSION

In this paper, we considered wireless-powered multicasting service for M2M devices in cellular networks. Multiple ETs are distributed in the network to transfer energy to the M2M devices. M2M devices utilize M2M communication to transfer multicast messages, and they are compensated for the energy consumed for forwarding the multicast messages. We formulated the problem mathematically, and the goal is to minimize the total transmitted energy by these ETs. The formulated problem is hard to solve since it is a non-convex MINLP. Therefore, we utilized GBD algorithm to decompose the problem into an NLP and an MILP subproblem. Then, we approximated the non-convex data rate function by a lower bound concave function and used SCP algorithm within GBD to solve the problem.

Because the problem is still hard to solve using GBD-SCP, especially when the number of binary variables is large, we proposed the CDR algorithm to solve the problem more efficiently. By utilizing the dependence of some variables on each other, we decomposed the original problem into three easier to solve sub-problems with binary variables relaxation. We studied the performance of CDR algorithm which achieves a performance that is close to GBD-SCP algorithm, but requires less computation time when the network size is large. We showed that the hybrid network architecture contributes to reducing the total transmitted energy by the ETs.

#### REFERENCES

[1] D. Lecompte and F. Gabin, "Evolved multimedia broadcast/multicast service (eMBMS) in LTE-advanced: Overview and Rel-11 enhancements," *IEEE Commun. Mag.*, vol. 50, no. 11, pp. 68–74, Nov. 2012.

- [2] A. Al-Fuqaha, M. Guizani, M. Mohammadi, M. Aledhari, and M. Ayyash, "Internet of Things: A survey on enabling technologies protocols and applications," *IEEE Commun. Surveys Tuts.*, vol. 17, no. 4, pp. 2347–2376, 4th Quart., 2015.
- [3] D. Evans, "The Internet of Things: How the next evolution of the Internet is changing everything," Cisco, San Jose, CA, USA, White Paper, 2011.
- [4] G. Araniti, M. Condoluci, P. Scopelliti, A. Molinaro, and A. Iera, "Multicasting over emerging 5G networks: Challenges and perspectives," *IEEE Netw.*, vol. 31, no. 2, pp. 80–89, Mar./Apr. 2017.
- [5] X. Lu, P. Wang, D. Niyato, D. I. Kim, and Z. Han, "Wireless networks with RF energy harvesting: A contemporary survey," *IEEE Commun. Surveys Tuts.*, vol. 17, no. 2, pp. 757–789, 2nd Quart., 2015.
- [6] D. Niyato et al., "Wireless powered communication networks: Research directions and technological approaches," *IEEE Wireless Commun.*, vol. 24, no. 6, pp. 88–97, Dec. 2017.
- [7] S. Wang, M. Xia, and Y.-C. Wu, "Multicast wirelessly powered network with large number of antennas via first-order method," *IEEE Trans. Wireless Commun.*, vol. 17, no. 6, pp. 3781–3793, Jun. 2018.
- [8] Z. Zhou et al., "Energy-efficient resource allocation for energy harvesting-based cognitive machine-to-machine communications," *IEEE Trans. Cogn. Commun. Netw.*, vol. 5, no. 3, pp. 595–607, Sep. 2019.
- [9] Z. Chu et al., "Resource allocation for secure wireless powered integrated multicast and unicast services with full duplex self-energy recycling," *IEEE Trans. Wireless Commun.*, vol. 18, no. 1, pp. 620–636, Jan. 2019.
- [10] K. Huang et al., "Enabling wireless power transfer in cellular networks: Architecture, modeling and deployment," *IEEE Trans. Wireless Commun.*, vol. 13, no. 2, pp. 902–912, Feb. 2014.
- [11] Q. Wu et al., "Energy-efficient resource allocation for wireless powered communication networks," *IEEE Trans. Wireless Commun.*, vol. 15, no. 3, pp. 2312–2327, Mar. 2016.
- [12] H. Tabassum *et al.*, "Wireless-powered cellular networks: Key challenges and solution techniques," *IEEE Commun. Mag.*, vol. 53, no. 6, pp. 63–71, Jun. 2015.
- [13] Z. Xie et al., "Wireless powered communication networks using peer harvesting," IEEE Access, vol. 5, pp. 3454–3464, 2017
- [14] A. Ercan M. O. Sunay, and I. F. Akyildiz, "RF energy harvesting and transfer for spectrum sharing cellular IoT communications in 5G systems," *IEEE Trans. Mobile Comput.*, vol. 17, no. 7, pp. 1680–1694, Jul 2018
- [15] Z. Yang W. Xu, Y. Pan, C. Pan, and M. Chen, "Energy efficient resource allocation in machine-to-machine communications with multiple access and energy harvesting for IoT," *IEEE Internet Things J.*, vol. 5, no. 1, pp. 229–245, Feb. 2018.
- [16] A. Almasoud and A. E. Kamal, "Efficient data and energy transfer in IoT with a mobile cognitive base station," in *Proc. IEEE Pers. Indoor Mobile Radio Commun. (PIMRC)*, 2017, pp. 1–5.
- [17] Y. Xiao et al., "Full-duplex machine-to-machine communication for wireless-powered Internet-of-Things," in Proc. IEEE Int. Conf. Commun. (ICC), Kuala Lumpur, Malaysia, Sep. 2016, pp. 1–6.
- [18] M. Condoluci et al., "Enabling the IoT machine age with 5G: Machinetype multicast services for innovative real-time applications," *IEEE Access*, vol. 4, pp. 5555–5569, 2016.
- [19] C. C. Kuan et al., "Reliable multicast and broadcast mechanisms for energy-harvesting devices," *IEEE Trans. Veh. Technol.*, vol. 63, no. 4, pp. 1813–1826, Apr. 2014.
- [20] J. Huang et al., "Multicast routing for multimedia communications in the Internet of Things," *IEEE Internet Things J.*, vol. 4, no. 1, pp. 215–224, Feb. 2017.
- [21] A. M. Geoffrion, "Generalized benders decomposition," J. Optim. Theory Appl., vol. 10, pp. 237–260, Oct. 1972.
- [22] F. Yuan et al., "Optimal harvest-use-store strategy for energy harvesting wireless systems," *IEEE Trans. Wireless Commun.*, vol. 14, no. 2, pp. 698–710, Feb. 2015.
- [23] C. A. Balanis, Antenna Theory: Analysis and Design. Hoboken, NJ, USA: Wiley, 2005, p. 68.
- [24] E. Boshkovska et al., "Practical non-linear energy harvesting model and resource allocation for SWIPT systems," *IEEE Commun. Lett.*, vol. 19, no. 12, pp. 2082–2085, Dec. 2015.
- [25] S. Wang et al., "Space-time signal optimization for SWIPT: Linear versus nonlinear energy harvesting model," *IEEE Commun. Lett.*, vol. 22, no. 2, pp. 408–411, Feb. 2018.
- [26] M. R. Garey et al., Computers and Intractability: A Guide to the Theory of NP-Completeness. New York, NY, USA: Freeman, 1979.
- [27] S. Boyd and L. Vandenberghe, *Convex Optimization*. Cambridge, U.K.: Cambridge Univ. Press, 2004.

- [28] R. Rosenthal, GAMS-A User's Guide, GAMS Develop. Corporat., Washington, DC, USA, 2007.
- [29] S. Vigerske and A. Gleixner, "SCIP: Global optimization of mixed-integer nonlinear programs in a branch-and-cut framework," *Optim. Methods Softw.*, vol. 33, no. 3, pp. 563–593, May 2018.
- [30] A. Brooke et al., GAMS/Cplex 7.0 User Notes, GAMS Develop. Corporat., Washington, DC, USA, 2000.
- [31] A. Wächter et al., "On the implementation of an interiorpoint filter line-search algorithm for large-scale nonlinear programming," Math. Program., vol. 106, pp. 25–57, May 2006.
- [32] D. Karolak et al., "Design comparison of low-power rectifiers dedicated to RF energy harvesting," in Proc. IEEE ICECS, Seville, Spain, Dec. 2012, pp. 524–527.
- [33] S. Agrawal et al., "Realization of efficient RF energy harvesting circuits employing different matching technique," in Proc. IEEE ISQED, Santa Clara, CA, USA, Mar. 2014, pp. 754–761.
- [34] P. Nintanavongsa *et al.*, "Design optimization and implementation for RF energy harvesting circuits," *IEEE J. Emerging Sel. Topics Circuits Syst.*, vol. 2, no. 1, pp. 24–33, Mar. 2012.



Abdullah M. Almasoud received the B.Sc. degree in computer engineering from King Saud University, Riyadh, Saudi Arabia, and the M.Sc. degree in computer engineering and the Ph.D. degree in computer engineering and electrical engineering from Iowa State University, Ames, IA, USA. He is currently an Assistant Professor with the Department of Electrical Engineering, Prince Sattam bin Abdulaziz University, Al-Kharj, Saudi Arabia. His research interests include wireless networks, cognitive radio networks, Internet of Things, UAV-

assisted networking, and RF energy harvesting. He was a recipient of the Best Paper Award at the IEEE Global Communications Conference 2018 on Ad Hoc and Sensors Networks Symposium.



Ahmed E. Kamal (Fellow, IEEE) received the B.Sc. (Distinction with Hons.) and M.Sc. degrees in electrical engineering from Cairo University, Egypt, and the M.A.Sc. and Ph.D. degrees in electrical engineering from the University of Toronto, Canada.

He is a Professor and the Director of graduate education with the Department of Electrical and Computer Engineering, Iowa State University, USA. His research interests include cognitive radio networks, optical networks, wireless sensor networks, and performance evaluation.

Prof. Kamal received the 1993 IEE Hartree Premium for papers published in Computers and Control in IEE Proceedings, and the Best Paper Awards of the IEEE Globecom Symposium on Ad Hoc and Sensors Networks Symposium in 2008 and 2018. He also received the 2016 Outstanding Technical Achievement Award from the Optical Networks Technical Committee of the IEEE Communications Society. He chaired or co-chaired Technical Program Committees of several IEEE sponsored conferences, including the Optical Networks and Systems Symposia of the IEEE Globecom in 2007 and 2010, the Cognitive Radio and Networks Symposia of the IEEE Globecom in 2012 and 2014, and the Access Systems and Networks track of the IEEE International Conference on Communications in 2016 and IEEE Globecom in 2020. He was also the Chair of the IEEE Communications Society Technical Committee on Transmission, Access and Optical Systems from 2015 to 2016. He serves or served on the editorial boards of a number of journals, including the IEEE Communications Magazine (a Lead Editor of the IEEE Communications Magazine Data Science and Artificial Intelligence for Communications Series), IEEE COMMUNICATIONS SURVEYS AND TUTORIALS, Computer Networks Journal (Elsevier), Optical Switching and Networking Journal (Elsevier), and the Arabian Journal of Science and Engineering. He was an IEEE Communications Society Distinguished Lecturer from 2013 to 2014. He is a Senior Member of the Association of Computing Machinery.